

# Scaling Human Activity Recognition: A Comparative Evaluation of Synthetic Data Generation and Augmentation Techniques

Zikang Leng

zleng7@gatech.edu

Georgia Institute of Technology

Atlanta, Georgia, USA

Archith Iyer

aiyer351@gatech.edu

Georgia Institute of Technology

Atlanta, Georgia, USA

Thomas Plötz

thomas.ploetz@gatech.edu

Georgia Institute of Technology

Atlanta, Georgia, USA

## Abstract

Human activity recognition (HAR) is often limited by the scarcity of labeled datasets due to the high cost and complexity of real-world data collection. To mitigate this, recent work has explored generating virtual inertial measurement unit (IMU) data via cross-modality transfer. While video-based and language-based pipelines have each shown promise, they differ in assumptions and computational cost. Moreover, their effectiveness relative to traditional sensor-level data augmentation remains unclear. In this paper, we present a direct comparison between these two virtual IMU generation approaches against classical data augmentation techniques. We construct a large-scale virtual IMU dataset spanning 100 diverse activities from Kinetics-400 and simulate sensor signals at 22 body locations. The three data generation strategies are evaluated on benchmark HAR datasets (UTD-MHAD, PAMAP2, HAD-AW) using four popular models. Results show that virtual IMU data significantly improves performance over real or augmented data alone, particularly under limited-data conditions. We offer practical guidance on choosing data generation strategies and highlight the distinct advantages and disadvantages of each approach.

## CCS Concepts

- Human-centered computing → Ubiquitous and mobile computing;
- Computing methodologies → Artificial intelligence.

## Keywords

Virtual IMU Data; Activity Recognition; Data Augmentation

## ACM Reference Format:

Zikang Leng, Archith Iyer, and Thomas Plötz. 2025. Scaling Human Activity Recognition: A Comparative Evaluation of Synthetic Data Generation and Augmentation Techniques. In *Proceedings of ACM Conference (Conference'17)*. ACM, New York, NY, USA, 8 pages. <https://doi.org/10.1145/nnnnnnnnnnnnnn>

## 1 Introduction

A persistent challenge in Human activity recognition (HAR) is the lack of large-scale, richly annotated IMU datasets. Collecting such data is costly and labor-intensive, requiring precise sensor placement, diverse participant recruitment, and manual labeling—often

---

Permission to make digital or hard copies of all or part of this work for personal or classroom use is granted without fee provided that copies are not made or distributed for profit or commercial advantage and that copies bear this notice and the full citation on the first page. Copyrights for components of this work owned by others than the author(s) must be honored. Abstracting with credit is permitted. To copy otherwise, or republish, to post on servers or to redistribute to lists, requires prior specific permission and/or a fee. Request permissions from [permissions@acm.org](mailto:permissions@acm.org).

*Conference'17, July 2017, Washington, DC, USA*

© 2025 Copyright held by the owner/author(s). Publication rights licensed to ACM.

ACM ISBN 978-x-xxxx-xxxx-x/YY/MM...\$15.00

<https://doi.org/10.1145/nnnnnnnnnnnnnn>

resulting in datasets with limited activity coverage and constrained sensor setups [7]. Consequently, models trained on these datasets tend to generalize poorly across users and environments, hindering real-world deployment [30].

To address the scarcity of labeled IMU datasets, recent work has explored cross-modality transfer techniques that generate virtual IMU data from more abundant sources such as video and text. Video-based methods like IMUTube [18, 19] transform 2D RGB activity videos—sourced from platforms like YouTube or datasets such as Kinetics-400 [16]—into virtual IMU signals through pose estimation and biomechanical signal modeling. In contrast, text-based pipelines such as IMUGPT [20, 22] leverage large language models (LLMs) and text-to-motion models like T2M-GPT [44] to synthesize human motion from natural language descriptions, producing semantically diverse virtual IMU data. While both approaches offer scalability far beyond conventional IMU datasets, they differ in their underlying assumptions and computational requirements.

Cross-modality transfer approaches can be understood as an alternative form of data augmentation that synthesizes new training examples from external modalities—such as text or video—rather than modifying existing IMU signals. By generating virtual IMU data that reflects diverse activity variations, these methods enrich the training data and can boost downstream HAR performance when used alongside real-world data. While both text-based and video-based pipelines have individually demonstrated benefits, they have only been evaluated in isolation. Currently, no study has directly compared these two approaches. Moreover, despite their shared objective with traditional sensor-level data augmentation, cross-modality methods have not been systematically benchmarked against them. This lack of comparative analysis leaves practitioners with limited guidance on how to choose between these strategies for improving HAR models.

In this paper, we compare these three methods for large-scale IMU data generation. Our results show that incorporating virtual IMU data consistently enhances model performance compared to training on real data alone or with traditional data augmentation—particularly when real data is scarce. Video-generated virtual IMU data generally provide more accurate motion information, while text-generated virtual IMU data contribute semantic and contextual diversity; combining both leads to the model with the best performance. Additionally, we find that virtual IMU data greatly benefit underrepresented activity classes and can help mitigate class imbalance. Our findings highlight the practical advantages of cross-modality transfer approaches and offer insights into how their complementary strengths can be leveraged for scalable HAR.

Our key contributions are:

- (1) We generate a large-scale virtual IMU dataset covering 100 diverse human activities from Kinetics-400, with simulated

signals at 22 *distinct sensor locations*. This dataset will be made publicly available upon acceptance.

- (2) We evaluate three data generation methods—classical sensor-level augmentation, video-based virtual IMU data generation using IMUTube, and text-based virtual IMU data generation using IMUGPT—on three HAR datasets: PAMAP2 [32], HAD-AW [25], and UTD-MHAD [4].
- (3) We provide practical guidelines for researchers and practitioners on selecting the most appropriate data generation technique based on resource constraints, desired activity complexity, and deployment scenarios.

## 2 Related Work

### 2.1 Human Activity Recognition

HAR has traditionally relied on the Activity Recognition Chain (ARC), which includes recording, signal processing, segmentation, feature extraction, and classification. Early methods employed classical machine learning models trained on handcrafted features derived from time- and frequency-domain statistics.

With the rise of deep learning, end-to-end models operating directly on raw sensor signals have become prevalent. Convolutional neural networks (CNNs) [26], long short-term memory networks (LSTMs) [8], and hybrid architectures such as DeepConvLSTM [29, 35], BiLSTM with attention [42], and transformer-based models [11] achieve state-of-the-art results by capturing local temporal dynamics, long-range dependencies, and inter-channel relationships.

However, these supervised DL approaches require substantial labeled data to perform effectively [30]. To mitigate this dependency, alternative learning paradigms have emerged. Self-supervised learning (SSL) frameworks pre-train models using auxiliary objectives—such as contrastive prediction or temporal ordering—before fine-tuning on limited labeled data [5, 6, 14, 27]. Transfer learning further extends model generalization by adapting representations learned in one domain or user group to new contexts [3, 10, 36].

Building upon these directions, our work investigates the effectiveness of cross-modality transfer techniques to generate virtual IMU data from alternative modalities.

### 2.2 Cross-Modality Transfer

Cross-modality transfer methods aim to address the scarcity of labeled IMU datasets by leveraging existing annotated datasets from other sensing modalities. The central idea is to convert data from a source modality—such as video [18, 19, 24, 33], text [20, 22], or motion capture [37, 38]—into virtual IMU signals.

A prominent example of a video-based method is IMUTube [18, 19], which converts 2D videos into virtual IMU data. It first extracts 2D and 3D human poses from the videos, then estimates joint rotations and full-body motion, from which virtual IMU signals are generated. This pipeline supports scalable data generation from publicly available video sources such as YouTube or large video datasets like Kinetics-400 [16]. The generated virtual IMU data has shown to significantly enhance the performance of downstream HAR models, particularly for activities involving large-scale movements such as locomotion or gym exercises. However, follow-up evaluations revealed that the benefits are more limited for activities involving subtle motions, such as driving [21].

In parallel, text-based approaches such as IMUGPT [20, 22] leverage LLMs to generate diverse textual descriptions of daily activities. Using a text-to-motion model, these textual descriptions are then converted into 3D motion sequences and subsequently into virtual IMU signals. The diversity in text prompts aims to reflect the wide range of ways in which humans perform activities in real life. Training models on this diverse set of virtual IMU signals can lead to improved generalizability and robustness in activity recognition.

Both video- and text-based approaches have shown promise in improving model performance, especially in scenarios where real IMU data is scarce or imbalanced. However, existing evaluations have examined these modalities in isolation, making direct comparisons difficult. This work provides the first head-to-head evaluation of video- and text-based virtual IMU generation methods under consistent experimental settings, enabling a more rigorous assessment of their relative effectiveness.

### 2.3 Data Augmentation

Data augmentation is a widely used strategy to improve model generalization by synthetically increasing the diversity of the training data. Whereas in computer vision common transformations include cropping, rotation, flipping, and color jittering [34], sensor-based HAR has adopted domain-specific augmentation techniques designed to perturb and thus enhance sensor signals.

Typical augmentations for IMU signals include axis permutation, adding Gaussian noise, temporal warping, signal scaling, and rotation transformations. These methods introduce controlled variations to the input signals and have been shown to improve model robustness to inter-subject and intra-subject variability [2, 9, 12, 26]. Beyond these traditional methods, some studies have explored the use of Generative Adversarial Networks (GANs) to synthesize entirely new sensor data as a form of data augmentation [15, 23]—yet, overall, only with moderate or no success.

In this study, we provide a direct comparison between classical data augmentation and two cross-modality transfer pipelines—IMUTube and IMUGPT—to assess their respective benefits for downstream HAR model performance.

## 3 Comparative Study of Cross-Modality Transfer and Data Augmentation

This paper presents a comparative study designed to evaluate three approaches for expanding training data in HAR: (1) text-based cross-modality transfer (IMUGPT); (2) video-based cross-modality transfer (IMUTube); and (3) classical sensor-level data augmentation. We generate large-scale virtual IMU datasets using (1) and (2) and compare their effectiveness against traditional augmentation techniques by training and evaluating four HAR models across three real-world datasets. Figure 1 gives an overview of our study.

### 3.1 Large Scale Virtual IMU Data Generation

To construct our large-scale labeled virtual IMU dataset, we leveraged the Kinetics-400 dataset [16] as our source of reference videos. Kinetics-400 contains 400 diverse human action classes, each represented by 200 to 700 video clips, which was originally collected to support training of video-based human action recognition models.

From the Kinetics-400 dataset, we selected a subset of 100 action classes to serve as the basis for our virtual IMU dataset, aiming to capture a diverse range of human activities while staying within our

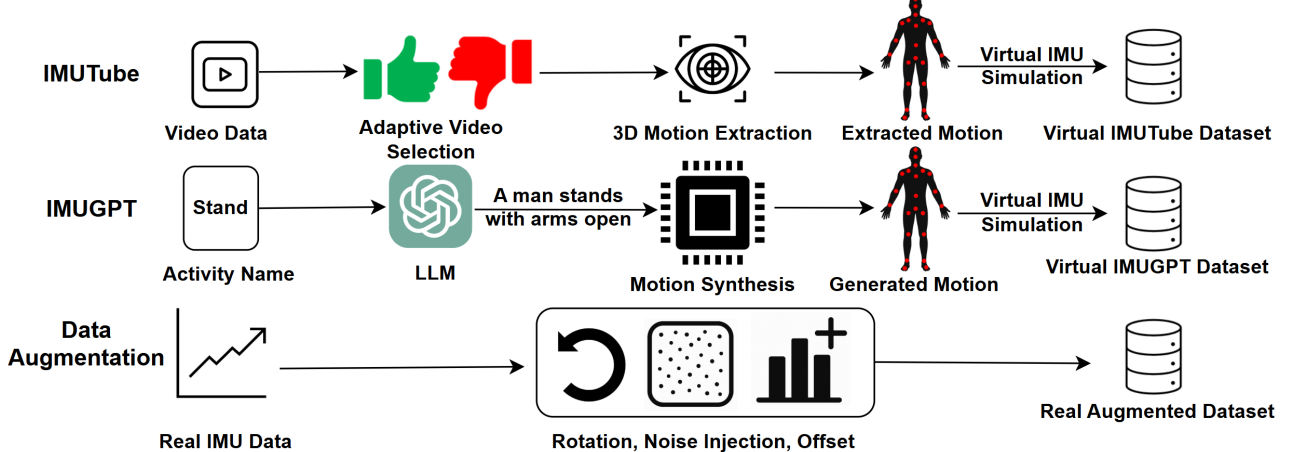


Figure 1: An overview of the three ways to scaling data.

computational constraints. To ensure a representative and balanced selection, we first grouped the 400 classes into broader semantic categories such as sports, daily activities, occupational tasks, and social interactions. Within each category, we then selected action classes that maximized overlap with activities commonly found in existing HAR datasets. This approach enabled us to focus on classes that are both semantically meaningful and relevant for sensor-based recognition.

To generate virtual IMU data for these activities, we employed two approaches: one based on textual descriptions and the other based on video inputs (details given below). We then compare the utility of the generated data from both approaches to improve the performance of downstream HAR models.

**3.1.1 Text-Based Virtual IMU Data Generation** To generate text-based virtual IMU data, we adopted the IMUGPT pipeline [20, 22], which can autonomously generate virtual IMU data by automatically generating natural language descriptions of human activities, and then converts the textual descriptions into 3D motion and, subsequently, virtual IMU data. The core idea is to capture the inherent variability in how activities are performed by first generating a diverse set of textual descriptions for each activity class, and then converting those into motion sequences.

For each activity, we used GPT-4o [28] to generate 500 short, varied descriptions ( $\leq 15$  words) that depict how the activity might be performed. The textual description generation process was guided by a few-shot prompting strategy, where we provided the LLM with example descriptions and high-level instructions (e.g., “the activity should involve only a single person, with minimal environmental detail”).

The generated textual descriptions were then passed to the motion synthesis model T2M-GPT [44] to produce 3D human motion sequences. T2M-GPT operates by first embedding the text using CLIP [31], then using the embedding, a transformer autoregressively generating code indices, which are subsequently decoded into latent vectors via a learned codebook. A learned decoder maps these latent representations into motion sequences consisting of

3D positions for 22 human body joints. Each generated textual description gets converted to a motion sequence (between five and ten seconds long), where the exact length depends on when the end token is generated by the transformer.

We estimated joint rotations using inverse kinematics [40], with the pelvis as the root joint following conventions in 3D human pose estimation. Using these rotations and the root joint’s translation, we simulated virtual IMU signals using IMUSim [41]. IMUSim computes linear acceleration and angular velocity for each joint, and introduces realistic sensor noise. Doing so, we generated virtual IMU data for 22 selected sensor locations across the body as shown in Figure 1. We refer to the resulting virtual IMU dataset as the Virtual IMUGPT dataset.

**3.1.2 Video-Based Virtual IMU Data Generation** To generate video-based virtual IMU data, we utilized the IMUTube pipeline [17, 18]. For each selected activity class, we sourced corresponding video clips from the Kinetics-400 dataset and processed them through IMUTube. Because many clips contain segments with occlusions, tracking errors, or unstable camera motion, we first applied an adaptive video selection module [19] to filter out low-quality segments. This module automatically removes sequences with irrelevant content, distorted or incomplete poses, obstructions, or significant foreground/background movement, ensuring that only segments suitable for pose tracking are retained.

The filtered video segments are then passed to the main IMUTube pipeline. First, 2D human poses are extracted from each frame using ViTPose [39], a transformer-based 2D pose estimation model. These 2D poses are then lifted into 3D using MixSTE [43], a state-of-the-art 3D pose estimation model. Next, camera ego-motion is estimated via 3D scene reconstruction techniques [45]. Combining the reconstructed 3D poses and estimated camera motion, IMUTube recovers the subject’s global movement trajectory in space.

As with IMUGPT, we use IMUSim [41] to simulate virtual IMU sensor readings. Virtual IMU data is extracted from 22 specified joint locations of the human body, as illustrated in Figure 1. From here on, we will refer to this generated dataset as the *Virtual IMUTube dataset*.

**Table 1: Training dataset sizes (in minutes).** IMUGPT and IMUTube refer to subsets of the virtual datasets containing only activities overlapping with each real dataset. Real Augmented denotes the size after applying data augmentation.

Datasets	Real	IMUGPT	IMUTube	Real Augmented
UTD-MHAD	21	544	196	85
PAMAP2	53	272	42	212
HAD-AW	399	943	255	1,595

### 3.2 Sensor-Level Data Augmentation

For a given segment of sensor data, we apply three forms of sensor-level data augmentation. Each segment is represented as a matrix  $\mathbf{X} \in \mathbb{R}^{T \times C}$ , where  $T$  is the number of samples in the segment and  $C$  is the total number of channels. Each tri-axial sensor contributes 3 channels, i.e.,  $C = 3S$ , where  $S$  is the number of sensors. The three forms of data augmentation that we applied are shown as follows:

(1) **Rotation Augmentation.** For each sensor  $s \in \{1, \dots, S\}$ , we extract the corresponding tri-axial data  $\mathbf{X}^{(s)} \in \mathbb{R}^{T \times 3}$  and apply a fixed rotation around the z-axis. The rotation matrix is defined as:

$$\mathbf{R}_z = \begin{bmatrix} \cos(\theta) & -\sin(\theta) & 0 \\ \sin(\theta) & \cos(\theta) & 0 \\ 0 & 0 & 1 \end{bmatrix}, \quad \text{with } \theta = \frac{\pi}{6}.$$

The rotated signal for each sensor is then computed as:

$$\mathbf{X}_{\text{rot}}^{(s)} = \mathbf{X}^{(s)} \cdot \mathbf{R}_z^\top.$$

All rotated sensor signals are concatenated to form  $\mathbf{X}_{\text{rot}} \in \mathbb{R}^{T \times C}$ .

(2) **Gaussian Noise Injection.** We add element-wise Gaussian noise sampled from  $\mathcal{N}(0, \sigma^2)$  with  $\sigma = 0.05$ , resulting in:

$$\mathbf{X}_{\text{noise}} = \mathbf{X} + \epsilon, \quad \epsilon \sim \mathcal{N}(0, 0.05^2).$$

(3) **Sensor Bias Simulation.** To emulate calibration drift or bias, we add a constant offset  $\mathbf{b} \in \mathbb{R}^{1 \times C}$ , where each component is sampled from the uniform distribution  $\mathcal{U}(-0.1, 0.1)$ .

The bias-augmented signal is:

$$\mathbf{X}_{\text{bias}} = \mathbf{X} + \mathbf{1}_T \cdot \mathbf{b},$$

where  $\mathbf{1}_T \in \mathbb{R}^{T \times 1}$  is a vector of ones to broadcast the bias across all timesteps.

For a given real IMU dataset, augmentation is applied to all segmented sensor windows obtained through a sliding window approach. The final training dataset includes  $\mathbf{X}$ ,  $\mathbf{X}_{\text{rot}}$ ,  $\mathbf{X}_{\text{noise}}$ , and  $\mathbf{X}_{\text{bias}}$ , which are concatenated along the batch dimension for training.

### 3.3 Datasets

We conducted our experiments using three publicly available HAR datasets: UTD-MHAD [4], PAMAP2 [32], and HAD-AW [25]. The UTD-MHAD dataset comprises recordings from eight subjects performing 27 activities, with each activity repeated four times per subject. IMU sensors were positioned on the right thigh for six lower-body activities and on the right wrist for the remaining 21 upper-body activities. The PAMAP2 dataset includes data from 9 subjects executing 18 different activities while wearing three IMU sensors placed on the chest, dominant wrist, and dominant ankle. The HAD-AW dataset contains recordings from 16 subjects who each performed 31 activities ten times while wearing an Apple Watch Series One on their right wrist.

**Table 2: Selected activity classes from each dataset that overlap with those available in Kinetics-400.**

Dataset	Selected Activity Classes
<b>HAD-AW</b>	Riding a bike, Dancing ballet, Drawing, Driving car, Eating burger, Playing piano, Playing guitar, Jogging, Using computer, Washing hands, Writing, Playing violin, Taking a shower, Making bed
<b>PAMAP2</b>	Walking, Jogging, Biking, Using computer, Folding clothes
<b>UTD-MHAD</b>	Clapping, Throwing ball, Shooting basketball, Drawing, Boxing, Hitting baseball, Hitting tennis ball, Push, Jogging, Walking, Squat

For each dataset, we selected only the activities that overlapped with those available in the Kinetics-400 dataset, ensuring that the generated virtual IMU datasets contains data for these activities. The final set of activities is listed in Table 2. We downsampled all real IMU recordings to 20 Hz to match the sampling rate of the virtual IMU data.

### 3.4 Experimental Settings

**3.4.1 Classification Models** We use four commonly adopted models in the HAR research community for our study: a Random Forest classifier, DeepConvLSTM [29], DeepConvLSTM with self-attention [35] and Bi-LSTM with attention [42]. To segment the IMU data, we apply a sliding window approach with a window size of two seconds and a one-second overlap between adjacent segments. The Random Forest model is trained on ECDF features [13], comprising 15 components extracted from the windows. DeepConvLSTM, DeepConvLSTM with self-attention, and BiLSTM with attention are trained directly on raw IMU signals for up to 30 epochs using the Adam optimizer, with learning rates dynamically adjusted via the ReduceLROnPlateau scheduler [1].

Hyperparameters, including learning rate (ranging from  $10^{-6}$  to  $10^{-2}$ ) and weight decay (from  $10^{-4}$  to  $10^{-3}$ ), are selected through grid search. For the UTD-MHAD and PAMAP datasets, we conduct leave-one-subject-out cross-validation for all three models. For the HAD-AW dataset, we instead employ 5-fold stratified cross-validation, as not all subjects performed the full set of activities in the released dataset. Cross-validation for each model is repeated three times using different random seeds, and we report the average macro F1 score along with the standard deviation across these runs.

**3.4.2 Training Configurations** We evaluate the following training configurations:

- (1) **Real Only:** The model is trained exclusively on the real IMU training dataset.
- (2) **Real + IMUGPT:** The training set consists of the real IMU training dataset combined with a subset of the Virtual IMUGPT dataset. The subset includes only data samples corresponding to the same activities and sensor locations as in the real dataset.
- (3) **Real + IMUTube:** Similar to the above, this configuration combines the real IMU training dataset with a subset of the Virtual IMUTube dataset, matched by activity types and sensor placements.

**Table 3: Comparison of Model Performance (Macro F1) using Full Real Data. Green shading indicates the best training configuration for each dataset and model combination.**

	UTD-MHAD	PAMAP2	HAD-AW
Random Forest Classifier			
Real Only	65.26 ± 0.34	48.09 ± 1.68	55.68 ± 0.22
Real + IMUGPT	63.41 ± 0.49	66.22 ± 2.34	53.19 ± 0.07
Real + IMUTube	66.65 ± 0.41	86.46 ± 2.38	54.64 ± 0.10
Real + IMUGPT + IMUTube	65.06 ± 0.51	88.35 ± 2.28	52.94 ± 0.27
Real + Augmentation	67.37 ± 0.62	47.60 ± 1.78	55.34 ± 0.19
DeepConvLSTM			
Real Only	51.36 ± 1.19	48.47 ± 9.11	66.53 ± 0.20
Real + IMUGPT	52.47 ± 0.29	74.01 ± 0.54	64.54 ± 0.16
Real + IMUTube	54.23 ± 0.21	82.48 ± 3.18	65.18 ± 0.37
Real + IMUGPT + IMUTube	52.09 ± 0.26	86.59 ± 0.88	63.85 ± 0.36
Real + Augmentation	57.33 ± 1.00	55.84 ± 0.31	67.15 ± 0.33
DeepConvLSTM with Self-Attention			
Real Only	51.86 ± 0.67	71.42 ± 1.81	67.79 ± 0.11
Real + IMUGPT	49.82 ± 0.52	84.31 ± 4.74	65.63 ± 0.23
Real + IMUTube	57.37 ± 0.46	82.64 ± 2.11	65.94 ± 0.30
Real + IMUGPT + IMUTube	49.30 ± 0.54	90.29 ± 0.65	64.65 ± 0.23
Real + Augmentation	58.26 ± 1.69	62.34 ± 4.71	67.71 ± 0.36
BiLSTM with Attention			
Real Only	78.57 ± 0.18	31.07 ± 2.43	89.49 ± 0.25
Real + IMUGPT	60.09 ± 1.49	47.90 ± 8.70	82.70 ± 0.28
Real + IMUTube	84.51 ± 1.99	52.39 ± 6.53	81.19 ± 0.30
Real + IMUGPT + IMUTube	64.33 ± 7.17	69.37 ± 9.88	81.28 ± 0.27
Real + Augmentation	78.82 ± 0.78	35.58 ± 3.81	89.51 ± 0.22

- (4) **Real + IMUGPT + IMUTube:** The model is trained on a combined dataset consisting of the real IMU data, along with subsets of both the Virtual IMUGPT and Virtual IMUTube datasets aligned in terms of activities and sensor locations.
- (5) **Real + Augmentation:** The training dataset includes only the real IMU training data, with data augmentation techniques applied.

For each training configuration, we additionally conducted experiments using only 10% of the real IMU training data to simulate scenarios where access to labeled IMU data is limited. In all cases, evaluation was performed on the unmodified real IMU test sets.

### 3.5 Results

Table 3 shows the model performances for the various training configurations when the full real IMU training dataset is used. When using the full real dataset, we find that incorporating the virtual IMU data—especially using the virtual IMUTube dataset or the combination of both virtual IMUTube and virtual IMUGPT datasets—generally leads to the most improvement in downstream model performance, particularly on PAMAP2 and UTD-MHAD.

- (1) **PAMAP2:** The combination of both virtual IMUTube and IMUGPT datasets yielded the most consistent performance gains. The DeepConvLSTM with Self-Attention model trained on Real + IMUGPT + IMUTube achieved the best macro F1 score of 90.29%, representing relative improvements of 26.4%, 44.83%, 7.1%, and 9.3% over training on Real Only,

**Table 4: Comparison of Model Performance (Macro F1) using 10% of the Real Data. Green shading indicates the best training configuration per dataset.**

	UTD-MHAD	PAMAP2	HAD-AW
Random Forest Classifier			
Real Only	36.13 ± 1.16	42.09 ± 4.89	33.88 ± 0.49
Real + IMUGPT	50.64 ± 0.38	77.22 ± 1.44	36.29 ± 0.37
Real + IMUTube	61.48 ± 0.69	85.30 ± 0.15	37.45 ± 0.37
Real + IMUGPT + IMUTUBE	60.65 ± 0.58	87.92 ± 2.01	39.23 ± 0.18
Real + Augmentation	53.82 ± 0.65	51.86 ± 7.35	33.80 ± 0.21
DeepConvLSTM			
Real Only	12.95 ± 1.19	28.72 ± 6.05	31.35 ± 0.05
Real + IMUGPT	30.71 ± 0.78	77.24 ± 2.27	34.58 ± 0.47
Real + IMUTube	36.40 ± 0.24	78.93 ± 2.02	37.86 ± 0.16
Real + IMUGPT + IMUTube	37.21 ± 0.44	91.08 ± 1.55	38.50 ± 0.38
Real + Augmentation	15.57 ± 4.12	39.57 ± 2.57	31.05 ± 0.04
DeepConvLSTM with Self-Attention			
Real Only	19.24 ± 0.22	37.34 ± 9.82	37.02 ± 0.35
Real + IMUGPT	29.39 ± 1.15	86.36 ± 3.16	36.88 ± 0.33
Real + IMUTube	40.92 ± 0.57	87.88 ± 0.16	40.52 ± 0.09
Real + IMUGPT + IMUTube	33.92 ± 0.41	90.27 ± 0.58	38.99 ± 0.19
Real + Augmentation	23.05 ± 1.66	54.07 ± 6.32	36.80 ± 0.48
BiLSTM with Attention			
Real Only	9.47 ± 0.90	20.90 ± 6.29	51.53 ± 0.30
Real + IMUGPT	12.61 ± 2.23	50.58 ± 3.02	45.81 ± 0.22
Real + IMUTube	37.42 ± 0.42	66.79 ± 7.16	52.88 ± 0.20
Real + IMUGPT+IMUTUBE	14.42 ± 1.22	59.64 ± 2.35	45.41 ± 0.25
Real + Augmentation	11.23 ± 0.55	28.43 ± 6.54	47.93 ± 0.28

Real + Augmentation, Real + IMUGPT, and Real + IMUTube, respectively.

- (2) **UTD-MHAD:** For the random forest classifier and DeepConvLSTM variants, training on Real + IMUTube and Real + Augmentation produced comparable performance. However, for the BiLSTM with Attention model, training on Real + IMUTube achieved the highest macro F1 score of 84.51%, with relative improvements of 7.6%, 7.2%, 40.6%, and 31.4% over Real Only, Real + Augmentation, Real + IMUGPT, and Real + IMUGPT + IMUTube, respectively.
- (3) **HAD-AW:** Performance was relatively stable across all training configurations. The addition of virtual IMU data or the application of data augmentation techniques did not yield significant improvements over using the unmodified real IMU data alone.

Table 4 summarizes the model performance across different training configurations when only 10% of the real IMU training dataset is used. Overall, incorporating virtual IMU data—particularly from the IMUTube dataset or using both virtual IMU datasets—leads to the most improvements across the models and datasets.

- (1) **PAMAP2:** The best performance was consistently achieved by models trained on Real + IMUGPT + IMUTube. For instance, the DeepConvLSTM model trained on this configuration reached the highest macro F1 score of 91.08%, showing relative improvements of 217.1%, 132.1%, 17.9%, and 15.4%

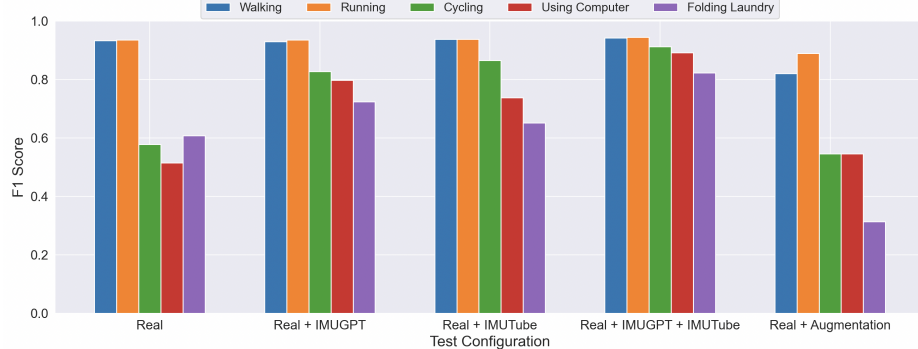


**Figure 2: Per-class macro F1 scores on the PAMAP2 dataset for the DeepConvLSTM with self-attention model under different training configurations.**

over Real Only, Real + Augmentation, Real + IMUGPT, and Real + IMUTube, respectively.

- (2) **UTD-MHAD:** Although the overall scores were lower due to the reduced real IMU training data, models trained with the virtual IMUTube dataset—either alone or in combination with virtual IMUGPT data—still outperformed other configurations. The Random Forest classifier trained on Real + IMUTube achieved the highest macro F1 score of 61.48%, representing relative improvements of 70.2%, 14.2%, 21.4%, and 1.4% over Real Only, Real + Augmentation, Real + IMUGPT, and Real + IMUGPT + IMUTube, respectively.
- (3) **HAD-AW:** Performance gains were more modest but consistent. Configurations using Real + IMUGPT + IMUTube or Real + IMUTube achieved the highest macro F1 scores across most models, suggesting that virtual IMU data becomes especially beneficial when real data is scarce.

## 4 Discussion

Across both full and limited (10%) real data training regimes, all three data expansion strategies—IMUTube, IMUGPT, and classical data augmentation—were evaluated against models trained on real IMU data only. Virtual IMU data generated via IMUTube and IMUGPT consistently led to substantial improvements in model performance across datasets and training conditions. In contrast, classical data augmentation produced mixed results and did not consistently outperform real-only baselines, highlighting the limitations of perturbation-based techniques in expanding data diversity.

*Cross-Modality vs. Classical Augmentation.* Cross-modality transfer techniques generally yielded larger performance gains than classical sensor-level data augmentation. On PAMAP2, for instance, combining virtual IMU data from both IMUGPT and IMUTube led to a 78% relative improvement in macro F1 over the real-only baseline using full data, compared to just a 4% gain with classical augmentation. In low-data conditions (10% real data), this performance gap widened further, with IMUGPT+IMUTube achieving 163.3% improvement versus 35.5% with augmentation. These results suggest that **cross-modality methods provide richer data diversity and semantics beyond what can be achieved by simple perturbations of existing signals.**

*IMUTube vs. IMUGPT.* Between the two virtual IMU data sources, IMUTube consistently delivered slightly better performance than IMUGPT, particularly on datasets with more complex physical activities. For example, on PAMAP2 with full data, Real+IMUTube provided a 58.08% gain versus 40.65% for Real+IMUGPT. This could be because video-based pose estimation can capture detailed and realistic motion from videos compared to text-based motion synthesis. Still, **using both IMUGPT and IMUTube together generally gave better results than using either one alone, showing that they complement each other—IMUGPT enriches diversity through diverse generated textual descriptions, while IMUTube provides accurate movement patterns.**

*Data Availability.* While all data expansion methods were beneficial under both full and limited real data regimes, their relative effectiveness was magnified in the 10% condition. Top-performing configurations achieved an average 116.9% boost over the Real Only baseline with 10% of the data, compared to a 28.8% improvement under full data. This underscores **the value of additional training data when the amount of real IMU data is limited.**

*Class Specific Improvement.* In addition to overall improvements, synthetic data notably enhanced performance on specific activity classes. Figure 2 presents per-class F1 scores for PAMAP2 across training configurations. We observed substantial gains for activities such as *biking*, *using computer*, and *folding clothes*, where real-only models performed poorly. These tasks involve motions that may be harder to generalize from limited real data. The addition of virtual IMU signals—particularly from IMUGPT, which introduces diverse activity descriptions—helped improve performance on these classes, suggesting that **virtual IMU data can help mitigate class imbalance or under-representation.**

*Computational Cost* From a deployment perspective, the computational cost of each method varies significantly. Classical data augmentation is computationally negligible. On Nvidia A6000, IMUGPT requires approximately 10 seconds to generate 10 seconds of virtual IMU data. In contrast, IMUTube takes approximately 5 minutes for the same output duration. Given these trade-offs, **we recommend IMUGPT as a practical starting point for practitioners with**

**limited computational or video resources. For those with access to greater resources, combining IMUTube and IMUGPT provides the most benefit and yields the most robust models.**

## 5 Conclusion

This paper presented a comparative study between classical data augmentation and two cross-modality transfer methods—IMUGPT and IMUTube—for virtual IMU data generation in HAR. We generated a large virtual IMU dataset spanning 100 activities and evaluated these methods across three datasets and four models. Results show that virtual IMU data consistently outperforms real-only and augmented baselines, especially in low-data regimes. IMUTube provides more accurate movement information, while IMUGPT contributes to broader data diversity; combining both often yields the best performance. Our findings offer practical guidance for selecting data generation strategies and highlight the value of virtual IMU data in scaling HAR.

## References

- [1] 2023. REDUCELRONPLATEAU. [https://pytorch.org/docs/stable/generated/torch.optim.lr\\_scheduler.ReduceLROnPlateau.html](https://pytorch.org/docs/stable/generated/torch.optim.lr_scheduler.ReduceLROnPlateau.html) (2024, Feb 1).
- [2] Luay Alawneh, Tamam Alsarhan, Mohammad Al-Zinati, Mahmoud Al-Ayyoub, Yaser Jararweh, and Hongtao Lu. 2021. Enhancing human activity recognition using deep learning and time series augmented data. *Journal of Ambient Intelligence and Humanized Computing* (2021), 1–16.
- [3] Sizhe An, Ganapati Bhat, Sutat Gunussoy, and Umit Ogras. 2023. Transfer learning for human activity recognition using representational analysis of neural networks. *ACM Transactions on Computing for Healthcare* 4, 1 (2023), 1–21.
- [4] Chen Chen, Roozbeh Jafari, and Nasser Kehtarnavaz. 2015. UTD-MHAD: A multimodal dataset for human action recognition utilizing a depth camera and a wearable inertial sensor. In *2015 IEEE International Conference on Image Processing (ICIP)*. 168–172. <https://doi.org/10.1109/ICIP.2015.7350781>
- [5] Hui Chen, Charles Gouin-Vallerand, Kévin Bouchard, Sébastien Gaboury, Mélanie Couture, Nathalie Bier, and Sylvain Giroux. 2024. Enhancing human activity recognition in smart homes with self-supervised learning and self-attention. *Sensors* 24, 3 (2024), 884.
- [6] Hui Chen, Charles Gouin-Vallerand, Kévin Bouchard, Sébastien Gaboury, Hubert Kenfack Ngankam, Maxime Lussier, Mélanie Couture, Nathalie Bier, and Sylvain Giroux. 2024. Utilizing Self-Supervised Learning for Recognizing Human Activity in Older Adults through Labeling Applications in Real-World Smart Homes. In *Proceedings of the 2024 International Conference on Information Technology for Social Good*. 275–283.
- [7] Wenqiang Chen, Shupei Lin, Elizabeth Thompson, and John Stankovic. 2021. SenseCollect: We Need Efficient Ways to Collect On-body Sensor-based Human Activity Data! *Proceedings of the ACM on Interactive, Mobile, Wearable and Ubiquitous Technologies* 5, 3 (2021), 1–27.
- [8] Yuwen Chen, Kunhua Zhong, Ju Zhang, Qilong Sun, and Xueliang Zhao. 2016. LSTM networks for mobile human activity recognition. In *2016 International conference on artificial intelligence: technologies and applications*. Atlantis Press, 50–53.
- [9] Ji Seok Choi and Jung Keun Lee. 2023. Effects of data augmentation on the nine-axis IMU-based orientation estimation accuracy of a recurrent neural network. *Sensors* 23, 17 (2023), 7458.
- [10] Sourish Gunesh Dhekane and Thomas Ploetz. 2024. Transfer learning in human activity recognition: A survey. *arXiv preprint arXiv:2401.10185* (2024).
- [11] Iveta Dirgová Luptáková, Martin Kubovčík, and Jiří Pospíšil. 2022. Wearable Sensor-Based Human Activity Recognition with Transformer Model. *Sensors* 22, 5 (2022). <https://doi.org/10.3390/s22051911>
- [12] Hassan Ismail Fawaz, Germain Forestier, Jonathan Weber, Lhassane Idoumghar, and Pierre-Alain Muller. 2018. Data augmentation using synthetic data for time series classification with deep residual networks. *arXiv:1808.02455 [cs.CV]* <https://arxiv.org/abs/1808.02455>
- [13] N. Y. Hammerla, R. Kirkham, P. Andras, and T. Ploetz. 2013. On preserving statistical characteristics of accelerometry data using their empirical cumulative distribution. In *Proceedings of the 2013 international symposium on wearable computers*. 65–68.
- [14] Harish Haresamudram, Irfan Essa, and Thomas Ploetz. 2022. Assessing the State of Self-Supervised Human Activity Recognition Using Wearables. *Proc. ACM Interact. Mob. Wearable Ubiquitous Technol.* 6, 3 (2022). <https://doi.org/10.1145/3550299>
- [15] Yifan Hu. 2023. Bsdgan: Balancing sensor data generative adversarial networks for human activity recognition. In *2023 International Joint Conference on Neural Networks (IJCNN)*. IEEE, 1–8.
- [16] Will Kay, Joao Carreira, Karen Simonyan, Brian Zhang, Chloe Hillier, Sudheendra Vijayanarasimhan, Fabio Viola, Tim Green, Trevor Back, Paul Natsev, Mustafa Suleyman, and Andrew Zisserman. 2017. The Kinetics Human Action Video Dataset. *arXiv:1705.06950 [cs.CV]* <https://arxiv.org/abs/1705.06950>
- [17] Hyekhyen Kwon, Gregory D Abowd, and Thomas Ploetz. 2019. Handling annotation uncertainty in human activity recognition. In *Proceedings of the 23rd International Symposium on Wearable Computers*. 109–117.
- [18] Hyekhyen Kwon, Catherine Tong, Harish Haresamudram, Yan Gao, Gregory D Abowd, Nicholas D Lane, and Thomas Ploetz. 2020. IMUTube: Automatic extraction of virtual on-body accelerometry from video for human activity recognition. *Proceedings of the ACM on Interactive, Mobile, Wearable and Ubiquitous Technologies* 4, 3 (2020), 1–29.
- [19] Hyekhyen Kwon, Bingyao Wang, Gregory D Abowd, and Thomas Ploetz. 2021. Approaching the Real-World: Supporting Activity Recognition Training with Virtual IMU Data. *Proceedings of the ACM on Interactive, Mobile, Wearable and Ubiquitous Technologies* 5, 3 (2021), 1–32.
- [20] Zikang Leng, Amitrajit Bhattacharjee, Hrudhai Rajasekhar, Lizhe Zhang, Elizabeth Bruda, Hyekhyen Kwon, and Thomas Ploetz. 2024. IMUGPT 2.0: Language-Based Cross Modality Transfer for Sensor-Based Human Activity Recognition. (2024). *arXiv:2402.01049 [cs.CV]*
- [21] Zikang Leng, Yash Jain, Hyekhyen Kwon, and Thomas Ploetz. 2023. On the Utility of Virtual On-body Acceleration Data for Fine-grained Human Activity Recognition. In *Proceedings of the 2023 ACM International Symposium on Wearable Computers (ISWC '23)*. Association for Computing Machinery, New York, NY, USA. <https://doi.org/10.1145/3594738.3611364>
- [22] Zikang Leng, Hyekhyen Kwon, and Thomas Ploetz. 2023. Generating Virtual On-Body Accelerometer Data from Virtual Textual Descriptions for Human Activity Recognition. In *Proceedings of the 2023 ACM International Symposium on Wearable Computers*. Association for Computing Machinery, New York, NY, USA. <https://doi.org/10.1145/3594738.3611361>
- [23] Xi'ang Li, Jinqi Luo, and Rabih Younes. 2020. ActivityGAN: Generative adversarial networks for data augmentation in sensor-based human activity recognition. In *Adjunct proceedings of the 2020 ACM international joint conference on pervasive and ubiquitous computing and proceedings of the 2020 ACM international symposium on wearable computers*. 249–254.
- [24] MinYen Lu, ChenHao Chen, Shigemi Ishida, Yugo Nakamura, and Yutaka Arakawa. 2022. A study on estimating the accurate head IMU motion from Video. *Proceedings of the Symposium on Multimedia, Distributed, Cooperative, and Mobile (DICOMO) 2022* (07 2022), 918–923. <https://cir.nii.ac.jp/crid/1050011771467456512>
- [25] Sara Mohammed, Reda Elbasiony, and Walid Gomaa. 2018. An LSTM-based Descriptor for Human Activities Recognition using IMU Sensors. 504–511. <https://doi.org/10.5220/0006902405040511>
- [26] Sebastian Münnzer, Philip Schmidt, Attila Reiss, Michael Hanselmann, Rainer Stiefelhagen, and Robert Dürichen. 2017. CNN-based sensor fusion techniques for multimodal human activity recognition. In *Proceedings of the 2017 ACM International Symposium on Wearable Computers (Maui, Hawaii) (ISWC '17)*. Association for Computing Machinery, New York, NY, USA, 158–165. <https://doi.org/10.1145/3123021.3123046>
- [27] Aaron van den Oord, Yazhe Li, and Oriol Vinyals. 2018. Representation learning with contrastive predictive coding. *arXiv preprint arXiv:1807.03748* (2018).
- [28] OpenAI, , Josh Achiam, Steven Adler, Sandhini Agarwal, Lama Ahmad, Ilge Akkaya, Florencia Leoni Aleman, Diogo Almeida, Janko Altenschmidt, Sam Altman, Shyamal Anadkat, Red Avila, Igor Babuschkin, Suchir Balaji, Valerie Balcom, et al. 2023. GPT-4 Technical Report. *arXiv:2303.08774 [cs.CL]*
- [29] Francisco Javier Ordóñez and Daniel Roggen. 2016. Deep Convolutional and LSTM Recurrent Neural Networks for Multimodal Wearable Activity Recognition. *Sensors* (2016).
- [30] Thomas Ploetz. 2023. If only we had more data!: Sensor-Based Human Activity Recognition in Challenging Scenarios. In *2023 IEEE International Conference on Pervasive Computing and Communications Workshops and other Affiliated Events (PerCom Workshops)*. 565–570. <https://doi.org/10.1109/PerComWorkshops56833.2023.10150267>
- [31] Alec Radford, Jong Wook Kim, Chris Hallacy, Aditya Ramesh, Gabriel Goh, Sandhini Agarwal, Girish Sastry, Amanda Askell, Pamela Mishkin, Jack Clark, Gretchen Krueger, and Ilya Sutskever. 2021. Learning Transferable Visual Models From Natural Language Supervision. In *Proceedings of the 38th International Conference on Machine Learning*, Vol. 139. PMLR, 8748–8763.
- [32] Attila Reiss and Didier Stricker. 2012. Introducing a New Benchmarked Dataset for Activity Monitoring (ISWC '12). IEEE Computer Society. <https://doi.org/10.1109/ISWC.2012.13>
- [33] Vitor Fortes Rey, Peter Hevesi, Onorina Kovalenko, and Paul Lukowicz. 2019. Let There Be IMU Data: Generating Training Data for Wearable, Motion Sensor Based Activity Recognition from Monocular RGB Videos. In *Adjunct Proceedings of the 2019 ACM International Joint Conference on Pervasive and Ubiquitous Computing and Proceedings of the 2019 ACM International Symposium on Wearable Computers*. Association for Computing Machinery, 699–708. <https://doi.org/10.1145/3341162>

3345590

[34] Connor Shorten and Taghi M Khoshgoftaar. 2019. A survey on image data augmentation for deep learning. *Journal of big data* 6, 1 (2019), 1–48.

[35] Satya P. Singh, Madan Kumar Sharma, Aimé Lay-Ekuakille, Deepak Gangwar, and Sukrit Gupta. 2021. Deep ConvLSTM With Self-Attention for Human Activity Decoding Using Wearable Sensors. *IEEE Sensors Journal* 21, 6 (2021), 8575–8582. <https://doi.org/10.1109/JSEN.2020.3045135>

[36] Elnaz Soleimani and Ehsan Nazerfard. 2021. Cross-subject transfer learning in human activity recognition systems using generative adversarial networks. *Neurocomputing* 426 (2021), 26–34.

[37] Lena Uhlenberg and Oliver Amft. 2022. Comparison of Surface Models and Skeletal Models for Inertial Sensor Data Synthesis. In *2022 IEEE-EMBS International Conference on Wearable and Implantable Body Sensor Networks (BSN)*. 1–5. <https://doi.org/10.1109/BSN56160.2022.9928504>

[38] Fanyi Xiao, Ling Pei, Lei Chu, Danping Zou, Wenxian Yu, Yifan Zhu, and Tao Li. 2021. A Deep Learning Method for Complex Human Activity Recognition Using Virtual Wearable Sensors. In *Spatial Data and Intelligence*. Springer International Publishing. [https://doi.org/10.1007/978-3-030-69873-7\\_19](https://doi.org/10.1007/978-3-030-69873-7_19)

[39] Yufei Xu, Jing Zhang, Qiming Zhang, and Dacheng Tao. 2022. ViTPose: Simple Vision Transformer Baselines for Human Pose Estimation. In *Advances in Neural Information Processing Systems*.

[40] K. Yamane and Y. Nakamura. 2003. Natural motion animation through constraining and deconstraining at will. *IEEE Transactions on Visualization and Computer Graphics* 9, 3 (2003), 352–360. <https://doi.org/10.1109/TVCG.2003.1207443>

[41] A. D. Young, M. J. Ling, and D. K. Arvind. 2011. IMUSim: A simulation environment for inertial sensing algorithm design and evaluation. In *Proceedings of the 10th ACM/IEEE International Conference on Information Processing in Sensor Networks*. 199–210.

[42] Junjie Zhang, Yuanhao Liu, and Hua Yuan. 2023. Attention-Based Residual BiLSTM Networks for Human Activity Recognition. *IEEE Access* 11 (2023), 94173–94187. <https://doi.org/10.1109/ACCESS.2023.3310269>

[43] Jinlu Zhang, Zhigang Tu, Jianyu Yang, Yujin Chen, and Junsong Yuan. 2022. MixSTE: Seq2seq Mixed Spatio-Temporal Encoder for 3D Human Pose Estimation in Video. In *Proceedings of the IEEE/CVF Conference on Computer Vision and Pattern Recognition (CVPR)*. 13232–13242.

[44] Jianrong Zhang, Yangsong Zhang, Xiaodong Cun, Shaoli Huang, Yong Zhang, Hongwei Zhao, Hongtao Lu, and Xi Shen. 2023. T2M-GPT: Generating Human Motion from Textual Descriptions with Discrete Representations. In *Proceedings of the IEEE/CVF Conference on Computer Vision and Pattern Recognition (CVPR)*.

[45] Wang Zhao, Shaohui Liu, Yezhi Shu, and Yong-Jin Liu. 2020. Towards Better Generalization: Joint Depth-Pose Learning without PoseNet. In *Proceedings of IEEE Conference on Computer Vision and Pattern Recognition (CVPR)*.